Quantification Issues in Arterial Spin Labeling Perfusion Magnetic Resonance Imaging

Wen-Chau Wu, PhD, Keith S. St Lawrence, PhD,† Daniel J. Licht, MD,‡ and Danny J.J. Wang, PhD§*

Abstract: Arterial spin labeling (ASL) perfusion magnetic resonance imaging has gained wide acceptance for its value in clinical and neuroscience applications during recent years. Its capability for noninvasive and absolute perfusion quantification is a key characteristic that makes ASL attractive for many clinical applications. In the present review, we discuss the main parameters or factors that affect the reliability and accuracy of ASL perfusion measurements. Our secondary goal was to outline potential solutions that may improve the reliability and accuracy of ASL in clinical settings. It was found that, through theoretical analyses, flow quantification is most sensitive to tagging efficiency and estimation of the equilibrium magnetization of blood signal (M_{0b}). Variations of blood T1 have a greater effect on perfusion quantification than variations of tissue T1. Arterial transit time becomes an influential factor when it is longer than the postlabeling delay time. The T2's of blood and tissue impose minimal effects on perfusion calculation at field strengths equal to or lower than 3.0 T. Subsequently, we proposed various approaches for in vivo estimation or calibration of the above parameters, such as the use of phase-contrast magnetic resonance imaging for calibration of the labeling efficiency as well as the use of inversion recovery TrueFISP (true fast imaging with steady-state precession) sequence for blood T1 mapping. We also list representative clinical cases in which implicit assumptions for ASL perfusion quantification may be violated, such as the venous outflow effect in children with sickle cell disease. Finally, an optimal imaging protocol including in vivo measurements of several critical parameters was recommended for clinical ASL studies.

Key Words: arterial spin labeling, perfusion, blood T1, water permeability

(*Top Magn Reson Imaging* 2010;21: 65–73)

Arterial spin labeling (ASL) perfusion magnetic resonance imaging (MRI) has gained wide acceptance for its value in clinical and neuroscience applications during recent years.[1] Compared with existing dynamic susceptibility contrast (DSC) methods, ASL has several unique advantages—it is an entirely noninvasive and highly economical technique that provides absolute quantification of perfusion. Its role in radiological health care is expected to grow further, given that ASL is a "green" and "renewable" technology with a superior cost-effectiveness ratio. Although signal-to-noise ratio (SNR) has been the main limiting factor for ASL in the past, recent technical advances in novel labeling schemes (eg, pseudocontinuous ASL [pCASL]) and readout sequences (eg, 3D), in conjunction with the growing availability of high magnetic fields and phased-array coils, have brought ASL to the frontier of practical clinical applications.[2] These technical advances and the risk of nephrogenic systemic fibrosis associated with DSC have led to a growing interest in using ASL to measure tissue perfusion in other organs, including lungs, kidneys, and heart.[3–6] This review mainly focuses on neurological applications as these remain the predominant focus of ASL studies.

Among the many appealing features of ASL, absolute perfusion quantification is a key characteristic that makes ASL attractive for many clinical applications. For instance, accurate measurement of perfusion plays a critical role in determining tissue viability in the clinical diagnosis and prognosis of stroke. Because perfusion is a well-characterized physiological parameter that is (theoretically) insensitive to scanning parameters, platform, field strength, and so on, ASL may offer an ideal tool for longitudinal studies to follow disease progression/recovery as well as to monitor therapy.[7] Quantitative methods such as ASL are being used more frequently in multisite studies that demand superior test-retest reliability of imaging techniques.[8] This has been the case in the recent multisite FBIRN study, in which a high variability of blood oxygenation level–dependent (BOLD) functional MRI (fMRI) data has been observed across sites and time.[9,10] In clinical neuroscience, a major challenge when interpreting BOLD fMRI data in patient populations is the potential for altered neurovascular coupling that may lead to spurious or undetected activation.[7] Quantitative perfusion may provide a more accurate and direct index of neuronal activity than BOLD fMRI, which reflects the complex interplay between blood flow, blood volume, and oxygen metabolism. Finally, ASL may complement the widely adopted BOLD contrast to improve the fidelity for inferring the underlying neuronal activity using fMRI.

General Schemes for ASL

Arterial spin labeling uses magnetically labeled arterial blood water as an endogenous tracer for measuring cerebral blood flow (CBF) or perfusion. In ASL experiments, inflowing arterial blood water is magnetically "tagged"—generally through inversion or saturation of the longitudinal magnetization—using specifically designed radiofrequency (RF) pulses. Image acquisition occurs after a delay in time to allow the labeled blood to flow into the imaging slices. Perfusion is determined by pairwise comparison of images that are acquired with labeling and without labeling (control). To improve the SNR of the perfusion images, repeated measurements of label and control are acquired over a few minutes.

According to the tagging scheme, ASL can be roughly divided into 3 categories: pulsed ASL (PASL),[11] continuous ASL (CASL),[12] and the newly introduced pCASL.[13–15] It is worth noting that alternative labeling schemes have been introduced such as velocity-selective labeling.[16] Pulsed ASL uses an instantaneous RF pulse (~10-20 milliseconds), whereas CASL

From the *Graduate Institute of Oncology and Graduate Institute of Clinical Medicine, National Taiwan University, Taipei, Taiwan; †Imaging Division, Lawson Health Research Institute, London, Ontario, Canada; ‡Division of Neurology, The Children's Hospital of Philadelphia, Philadelphia, PA; and §Department of Neurology, University of California Los Angeles, Los Angeles, CA.

Reprints: Danny J.J. Wang, PhD, Ahmanson-Lovelace Brain Mapping Center, UCLA Department of Neurology, 660 Charles E. Young Dr South, Los Angeles, CA 90095 (e-mail: jwang71@gmail.com).

This work was supported by National Institutes of Health grants MH080892, RR002305, AG016570-11A; Thrasher Research Fund; the Steve & June Wolfson Family Foundation; the Dana Foundation; and National Science Council grant NSC97-2314-B-002-172-MY3.

uses long RF pulses lasting for a few seconds. In pCASL, a train of discrete short RF pulses is used to mimic the long continuous tagging in CASL. Whereas the long labeling pulses in CASL and pCASL reduce physiological modulations,[17] PASL is amenable to shorter repetition time acquisition and thus better temporal resolution.[18] Whereas pCASL and PASL can be implemented with the standard body-coil transmission and phased-array reception on commercial magnetic resonance (MR) systems, CASL requires a dedicated coil with capacity of generating continuous RF pulses. When tagging efficiency and coil configuration are considered together, the SNR is comparable between PASL and CASL and is highest with pCASL, although pseudocontinuous tagging is more sensitive to field inhomogeneity and deposits a relatively high level of power.[14]

Perfusion Quantification Using ASL

In ASL experiments, magnetically tagged arterial blood first travels through major arteries and arterioles—the duration of which is termed arterial transit time. Once reaching capillaries, the labeled blood water rapidly diffuses into the surrounding tissue during its transit through the microvascular bed. The fraction of labeled water eventually "trapped" in tissue is a complicated function of blood flow, the capillary volume, and permeability of the endothelium to water. The remaining labeled water in the blood will flow out into venules and veins. This fraction is expected to be small at typical CBF values in humans because of the rapid T1 relaxation of the label (Fig. 1). Therefore, there is a certain level of similarity between ASL and microsphere-based blood flow measurements.[19]

In a simple sense, CBF can be quantified and expressed in units of milliliters per 100 g per minute by taking into account T1 relaxation of labeled blood. For instance, many existing ASL studies assume that the label follows a monoexponential decay with the blood T1 (ie, the labeled blood never exchanges into tissue).[20] A more accurate perfusion model consists of 2 serial compartments—arterial and tissue, due to the change from the T1 of blood to the T1 of tissue once the tracer exchanges out of capillaries.[21,22] Because water exchange does not occur instantly

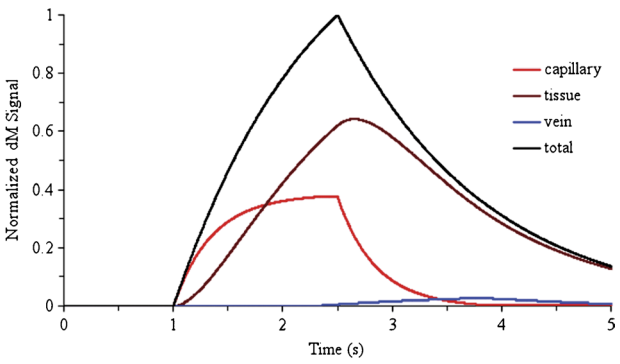

FIGURE 1. Predicted signal contributions from labeled water in the capillary, venous, and tissue spaces. Curves were generated using the SPA model[26] for the following parameters: CBF = 70.0 mL/100 g per minute, PS = 200 mL/100 g per minute, capillary blood volume = 1.5 mL/100 g, venous blood volume = 2.0 mL/100 g, $T1_{blood}$ = 1.49 seconds, $T1_{gray\ matter}$ = 1.26 seconds, arterial transit delay = 1.0 seconds, and CASL with a labeling period of 1.5 seconds. All curves were normalized to the maximum total signal. The largest venous contribution was 7% at approximately 4 seconds. Figure 1 can be viewed online in color at www.topicsinmri.com.

in the central nervous system, advanced tracer kinetic models have been developed that take into account limited water permeability across the blood-brain barrier (BBB).[23–26] These models can include up to 4 compartments: 2 nonexchanging compartments, that is, arteries and veins, and 2 exchanging compartments, that is, capillaries and tissue.[27]

During the past decade, validation studies of ASL in healthy human subjects have yielded encouraging results. Cerebral blood flow measurements with ASL perfusion MRI have been shown to agree with results from ^{15}O-PET (positron emission tomography) in healthy humans at rest[28] or during functional activation,[29] and with the DSC approach.[30–32] In addition, ASL perfusion measurements both at rest and during task activation have been demonstrated to be reproducible across intervals, varying from a few minutes to a few days.[33–36] However, potential variations of physiological and biophysical parameters in patient populations and across different age groups pose challenges for accurate perfusion quantification using ASL. The purpose of the present article was therefore to discuss the main parameters or factors that affect the reliability and accuracy of ASL perfusion measurements. Our secondary goal was to outline potential solutions that may improve the reliability and accuracy in clinical settings.

Theoretical Analysis of Modeling Errors

As the first step, it is helpful to determine the most "influential" parameters that affect perfusion quantification using ASL. The following is the analytic solution for calculating perfusion, f, in a typical CASL or pCASL experiment[22]:

$$f = \frac{\Delta M\ \exp(-TER_{2b})}{-2\alpha M_{0b}} \Bigg/ \left\{ \begin{array}{l} [\exp(-wR_{1b}) - \exp\left(\left(\min(\delta - w, 0) - \delta\right)R_{1b}\right)]\exp(-TER_{2b})/R_{1b} + \\ \exp(-\delta R_{1b})\left\{\frac{\exp(-wR_{1t})}{R_{1t}}[1 - \exp\left(\min(\delta - \tau, 0)R_{1t}\right)] + \right. \\ \left. \frac{1}{R_{1t}}[\exp\left(\min(\delta - w, 0)R_{1t}\right) - \exp(-wR_{1t})]\right\}\exp(TER_{2t}) \end{array} \right\} \quad [1]$$

where ΔM is the measured difference signal between label and control acquisitions. This equation takes into account the different longitudinal and transverse relaxation rates of blood and tissue (R_{1b} and R_{1t}; R_{2b} and R_{2t}), labeling efficiency (α), arterial transit time (δ), duration of the labeling pulse (τ), postlabeling delay time (w), and the equilibrium magnetization of blood signal (M_{0b}). We applied partial derivative analysis to illustrate the potential error in perfusion caused by 10% change in each of the above parameters in Equation [1], respectively. Table 1 lists the results of theoretical analyses, which show that flow quantification is most sensitive to tagging efficiency and M_{0b} estimation. Variations of blood T1 ($1/R_{1b}$) have a greater effect on perfusion than variations of tissue T1 ($1/R_{1t}$). As expected,[21] arterial transit time becomes an influential factor when it is longer than the postlabeling delay. The T2's of blood and tissue impose minimal effects on perfusion calculation at the assumed field strength of 3.0 T. In the following, we discuss the effect of each parameter on the accuracy of perfusion quantification, respectively.

Effect of Labeling Schemes on Quantification

As mentioned earlier, pCASL is a novel labeling scheme that combines the advantages of PASL and CASL. Experimental data in healthy adults using pCASL showed a 50% increase of SNR compared with PASL and a higher tagging efficiency than CASL (85% vs 68%).[14] Pseudo-CASL is expected to improve the reliability and accuracy of CBF measurements especially under conditions of low perfusion. To assess the performance of ASL perfusion imaging techniques in the pediatric population, we studied 12 children (age range, 4 days to 3 years) with congenital heart defects (CHDs) before and after hypercarbia, using

TABLE 1. Estimation of Quantitative Variability When the Imaging or Physiological Parameters Are 10% Larger Than Their True Values

	R_{1b}	R_{1t}	R_{2b}	R_{2t}	α	δ	M_{0b}
$\delta < w$	−7.2	−6.8	1.2	−3.0	11.1	1.7	11.1
$w < \delta$	−7.1	−3.2	0.9	−2.3	11.1	3.8	11.1

Seven parameters were considered one at a time, and the assigned values were: $R_{1b} = 1/1600\ ms^{-1}$, $R_{1t} = 1/1300\ ms^{-1}$, $R_{2b} = 1/150\ ms^{-1}$, $R_{2t} = 1/60\ ms^{-1}$, $\alpha = 0.9$, $\delta = 1200$ ms, $\tau = 1500$ ms, TE = 18 ms. Quantitative variability was calculated by comparing the estimated flow to the true flow: $\frac{flow^{Est} - flow^{True}}{flow^{True}} \times 100\%$.

both PASL and pCASL. Figure 2 shows CBF maps acquired using pCASL and PASL in a representative CHD child (4 days, male), whereas Figure 3 compares the mean CBF values (*a*) and the performance of these 2 techniques (*b*), as measured by percent negative voxels seen in the imaging planes. As can be seen, mean CBF values obtained with the 2 techniques generally match each other. Nevertheless, pCASL offers improvement in SNR and provides a more robust measure of CBF at low flows, as demonstrated by the reduced number of negative voxels using pCASL compared with PASL. Another advantage of pCASL is that the labeling plane is relatively uniform across subjects with different head sizes, whereas the labeling bolus in PASL may be variable in different age groups and has been demonstrated to be a confounding factor for measuring perfusion in infants.[37] Given its compatibility with array receive coils and superior performance, pseudo-CASL is expected to see growing clinical applications in the coming years. The only drawback of pCASL is the relatively high RF power it requires for spin labeling. However, our experience to date with this technique has been successful on commercial MR systems at 1.5 and 3.0 T.

Variations of Tagging Efficiency

As demonstrated by our theoretical analyses, tagging efficiency (α) is a direct scaling factor for calculating CBF. Uncertain α causes systematic error in individual measurement and increases variability between subjects and in longitudinal studies. In general, α is adopted from literature values; for example, α is approximately 95% for PASL,[38] 85% for pCASL,[14] and 70% for CASL.[12,39] Flow velocity and field inhomogeneity may cause suboptimal α, particularly for CASL and pCASL. One can calibrate α by conducting a dynamic phase contrast (PC) MRI over a cardiac cycle at the feeding arteries within the labeling plane. For instance, the total CBF volume (mL/min) to the brain can be estimated by the product of the velocity-time curve derived from PC MRI and the cross-sectional areas of the internal carotid arteries and vertebral arteries. With estimate of the brain volume (eg, from structural MRI), one can correlate the total blood flow obtained using PC MRI and ASL, thereby providing an effective means for calibrating α. A recent pCASL study in healthy adults using PC MRI as calibration indicated a mean tagging efficiency of 85%,[40] nicely matching our computer simulations that predicted an optimal tagging efficiency of 85% for flow velocity from 10 to 60 cm/s. In a recent study in healthy children aged 7 to 17 years, global CBF measurements using pCASL have been validated using PC MRI with a high intraclass correlation coefficient of 0.77.[41] It is worth noting that an alternative trend in the field is to apply autocalibration algorithms for deriving quantitative CBF, such as the model-free deconvolution approach proposed by Petersen et al.[42]

Arterial Transit Delays

Arterial transit artifact, manifested as focal intravascular signals in ASL images, is a major confounding factor for perfusion quantification. These artifacts result from intravascular label that has not reached capillaries and tissue by the time image acquisition is carried out. A few factors can affect the transit time, such as physiology, pathophysiology, and anatomy. For example, transit time can be substantially elongated in patients

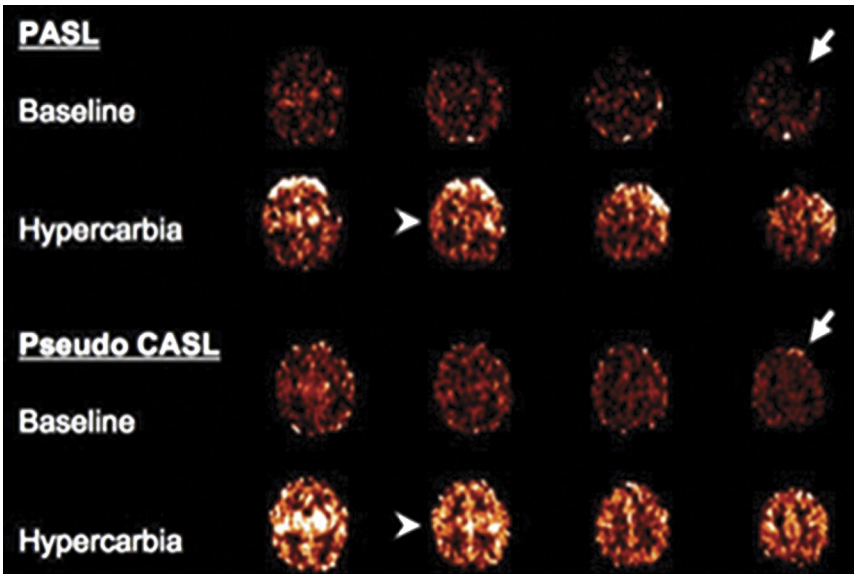

FIGURE 2. A direct comparison of PASL (upper) and pCASL (lower) in a child with CHD both at rest (baseline) and during hypercarbia. The 2 right arrows demonstrate increased negative pixels on PASL imaging, in the left frontal cortex. The arrowheads on the left demonstrate improved anatomic resolution in the central sulcus. Figure 2 can be viewed online in color at www.topicsinmri.com.

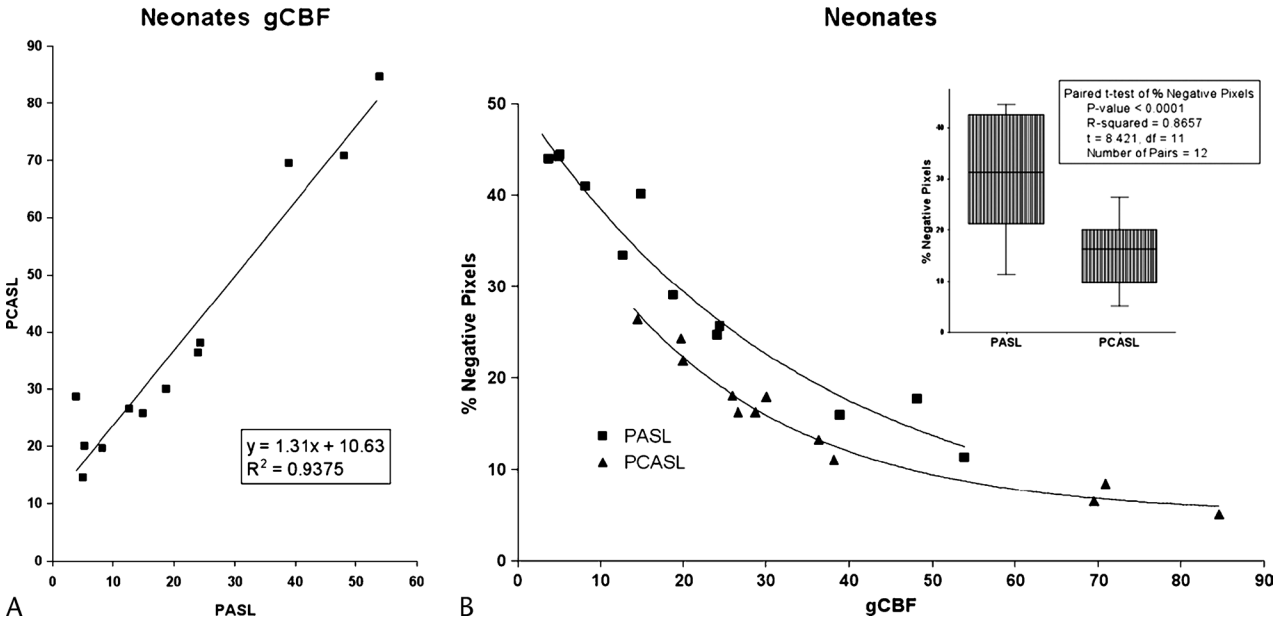

FIGURE 3. Direct comparison of mean global CBF values acquired using PCASL and PASL perfusion MRI in a cohort of infants and children with CHD (A). The percentage of negative voxels is plotted as a function of mean CBF values (B). With increased values of CBF, the percentage of negative voxels is reduced. Pseudo-CASL offers an improvement in SNR at low blood flow values.

with cerebrovascular diseases because of collateral circulation.[32] In fMRI studies, it has been shown that transit time decreases during task activation.[43] In extremity muscles, the transit time can be longer than 2 seconds.[44] When postlabeling delay time is too short, ASL measurement is biased toward arteries and arterioles, whereas tissue perfusion is underestimated. Although a long postlabeling delay can be applied to allow the label sufficient time to flow into capillaries and tissue, it reduces the SNR. In the brain, transit delay may distribute over a wide range (several tens of milliseconds) even within 1 imaging slice, which, if not accounted for, leads to erroneous flow quantification.

The choice of the optimal postlabeling delay time in clinical ASL applications is an empirical decision by the investigator as the tradeoff between minimizing transit artifacts and maximizing SNR.[20] However, such decision making may be difficult, given the variability of arterial transit times in patients with cerebrovascular disease.[45] Lately, there have been several new developments in the field that may provide robust perfusion measurements in the presence of prolonged transit delays. One approach is to map the arterial transit time in vivo because transit time per se is a clinically meaningful physiological parameter that may indicate vascular reserve. We have introduced such a technique termed FEAST (flow encoding arterial spin tagging) that uses 2 ASL scans with and without flow spoiling bipolar gradients, the ratio of which provides an estimate of arterial transit time.[46] An alternative approach is to simultaneously fit arterial transit time and perfusion through continuous sampling of the dynamic inflow of the label, often using the Look-Locker approach.[42,47] Because of the use of small flip angles, the SNR of Look-Locker–based ASL is lower with smaller image coverage compared with standard ASL acquisitions. Nevertheless, the feasibility of this approach in stroke imaging has been demonstrated.[48]

Figure 4 shows the comparison of FEAST and Look-Locker–based pCASL scans in a 7-year-old girl. The dynamic time courses of the inflowing bolus acquired using Look-Locker EPI–based pCASL reveal that the labeled bolus flows into microvasculature after a delay of 1000 milliseconds (when focal intravascular signals disappear). Correspondingly, the transit time generated using the FEAST technique ranges from approximately 1150 to 1550 milliseconds from he bottom to the top slice, with a mean of 1350 milliseconds. More recently, some investigators realized that arterial transit time maps may be intrinsically smooth in space and can be acquired with lower spatial resolution at high imaging speed (~1 minute). These "coarse" transit maps can then be used for determining the optimal postlabeling delay time for accurate perfusion quantification.[49]

T1 and T2 of Blood and Tissue

The T1 of blood and tissue is another important factor affecting the accuracy of ASL perfusion measurements. Strictly speaking, the tracer relaxation time shifts from blood T1 to tissue T1 once the labeled blood exchanges out of blood vessels. For simplicity, the 2 compartments may be merged into one when they have similar R_1 and R_2 values. Parkes and Tofts[24] reported that assigning the single compartment to tissue (ie, infinite permeability) led to perfusion overestimation (in the brain, 20% for gray matter and 60% for white matter). Alternatively, the single compartment can be assigned to blood. If the acquisition window is placed after the tagged protons arrive at the capillary network and before they diffuse into extravascular space, the single blood compartment model offers a simple and yet good estimate of perfusion without the need of T_1 measurement for tissue. It is therefore critical to obtain in vivo measurement of blood T1 as part of an ASL experiment. Recently, we have developed an ultrafast pulse sequence (<1 minute) based on inversion-recovery trueFISP (true fast imaging with steady-state precession) to measure venous blood T1 in the sagittal sinus.[50] Our data demonstrated a trend of decreasing blood T1 with age and higher values in females compared with males (Fig. 5). If left unaccounted for, the intersubject variations in blood T1 will be propagated into the estimated CBF. Previous ASL studies have

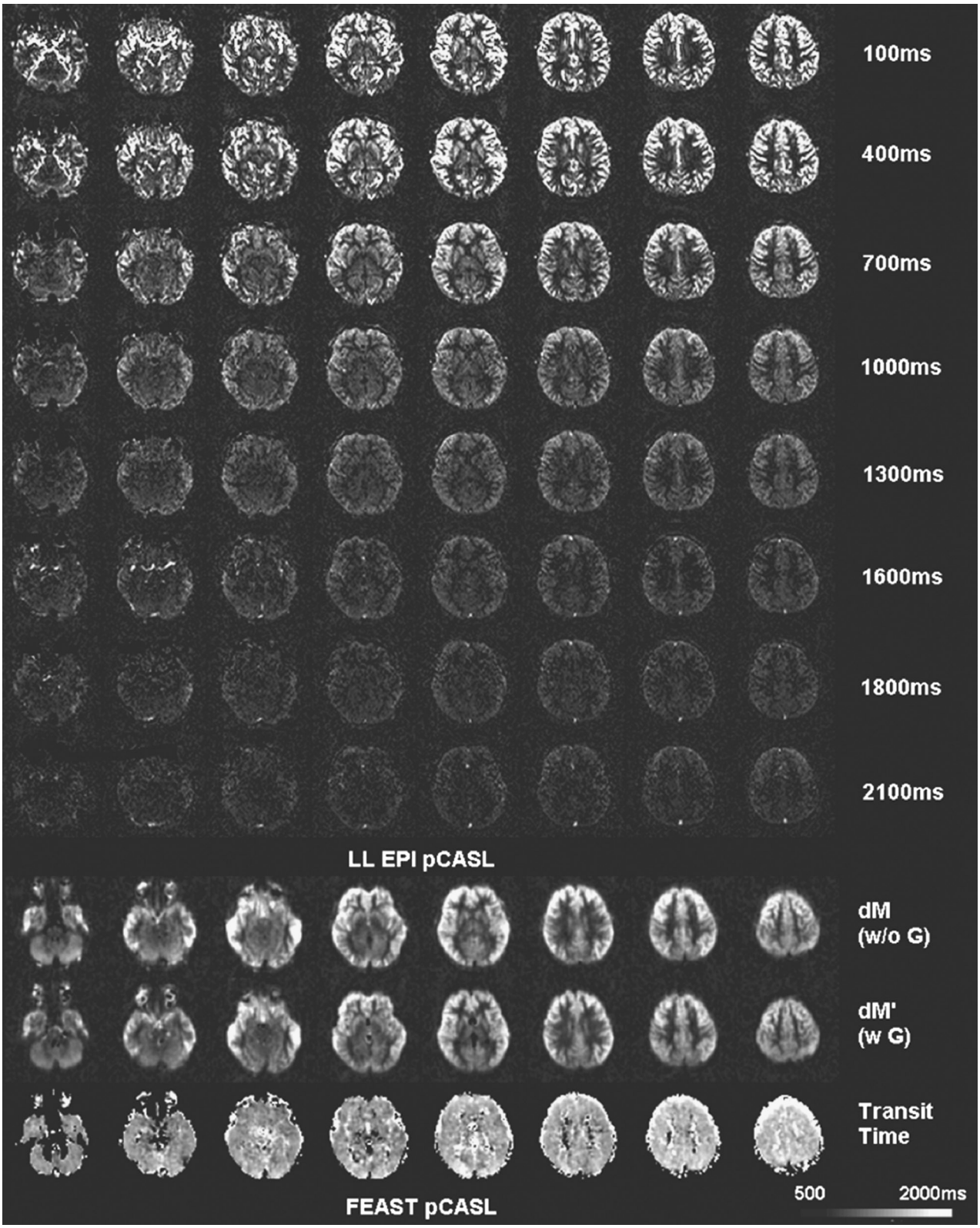

FIGURE 4. Series of pCASL images acquired using Look-Locker EPI from the delay of 100 to 2100 milliseconds with a temporal solution of 300 milliseconds (top 8 rows). The dynamic time courses of the inflowing bolus show the labeled bolus flows into microvasculature after a delay of 1000 milliseconds. The bottom 3 rows demonstrate the FEAST technique—transit time maps (range, 1150–1550 milliseconds from bottom to top slice with a mean of 1350 milliseconds) are generated by 2 pCASL images (dM′ and dM) acquired with and without flow spoiling gradients. Data were acquired from a 7-year-old girl.

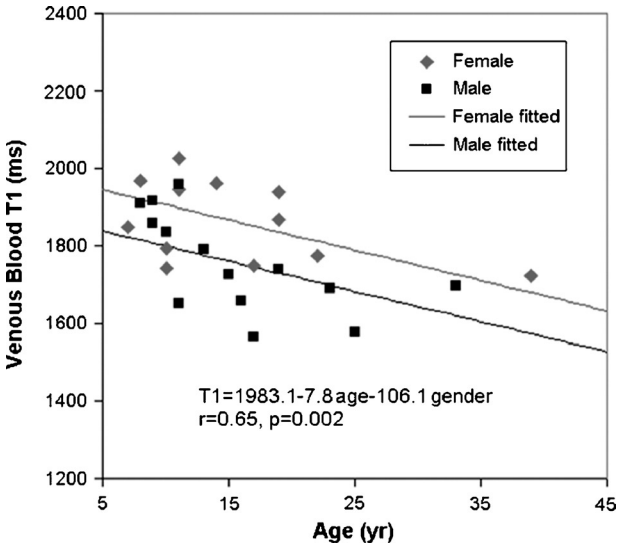

FIGURE 5. Measured blood T_1 as a function of age and sex with fitted lines for each sex in 26 children and adults aged 7 to 39 years (shallow diamond and line = female; dark square and line = male; sex = 0 for female and 1 for male). Figure 5 can be viewed online in color at www.topicsinmri.com.

also included in vivo measurement of tissue T1 as part of the scanning protocol.[36] However, the additional scan time and potential patient motion between T1 and ASL scans are existing obstacles for calibrating T1 effects on a pixel-by-pixel basis especially for clinical studies.

The T2 or T2* of blood and brain tissue can also affect perfusion measurement, although to a lesser extent than the T1 effect discussed above. At magnetic field strength equal to or lower than 3.0 T, transverse relaxation effects can be ignored because the echo time in ASL scans is generally much shorter than the T2/T2* of blood and brain tissue. At high and ultrahigh magnetic fields greater than 4.0 T, the T2/T2* of capillary blood is comparable to typical TE values. As a result, a significant amount of ASL signal may be dephased, leading to underestimation of CBF at high and ultrahigh fields (Fig. 6).[51] These data demonstrate the importance for using fast imaging sequences with ultrashort TE for high-field ASL, as well as the importance of accounting for susceptibility effects on perfusion quantification. On the other hand, the TE dependences of ASL and tissue signals may be used for estimation of tissue oxygenation. As shown in Figure 6, the fitted venous T2* may provide a surrogate index of venous oxygen saturation.

Water Permeability

Compared with contrast agents, water is a relatively freely diffusible tracer. Consequently ASL CBF measurements are not very sensitive to permeability changes of the BBB.[52] This may serve as an advantage of ASL for absolute perfusion quantification in tumor imaging as compared with DSC perfusion MRI, where a preload of contrast agent or compensation algorithms need to be applied.[53] On the other hand, permeability of the BBB is an important physiological parameter that may have clinical implications in aging, dementia, and cancer. The lack of sensitivity of ASL to permeability changes may ultimately serve as a disadvantage compared with DSC. Fortunately, emerging technologies are starting to address this important issue. We have recently developed a diffusion-weighted ASL technique that differentiates capillary and tissue fractions of labeled water based on their different diffusion characteristics (ie, high pseudodiffusion in capillaries and low diffusion coefficient in tissue). The ratio between the 2 compartment signals provides an estimate of water permeability based on a tracer kinetic model that accounts for water exchange between capillaries and tissue.[54] Nevertheless, this technique awaits clinical validation in future studies.

Venous Outflow

An implicit assumption in most existing quantitative models is that the tagged blood arrives at the capillary network and the surrounding tissue without leaving prior to data acquisition. Although this assumption generally holds in the brain of adult humans under normal conditions (Fig. 1), evidence has suggested a finite permeability of the capillary wall to water and, in turn, the increased likelihood that the tagged spins are able to pass through the capillary network without extraction into the tissue. Both elevated flow and prolonged tracer half-time (blood T1) may accentuate the venous outflow. In a recent study,[55] we applied CASL to measure perfusion in normal adults, normal children, and children with sickle cell disease (SCD). Healthy children are known to have increased CBF compared with adults, which is further elevated in children with SCD because of their decreased hematocrit level.[56,57] Venous outflow was identified as hyperintensities in the sinuses of the dura mater and further quantified as a function of the average flow in gray matter. Hyperintensities in the sagittal sinuses were observed in 20 of 24 children with SCD, 13 of 30 healthy children, and none of the young adults, indicating that the occurrence is associated with groups (χ^2 test, $P < 0.001$).

Figure 7A shows the CBF images obtained from 3 representative subjects (top row: a child with SCD; middle row: a healthy child; bottom row: a healthy adult). It is apparent that both global perfusion and hyperintentsities in the sagittal sinus (arrows) increased from the adult to the healthy child and to the child with SCD. In Figure 7B, the outflow effect is plotted against gray matter flow for both healthy children and children with SCD. In the latter, the outflow effect is found to positively correlate with perfusion. This venous outflow effect, if not properly accounted for, can lead to flow underestimation in ASL.

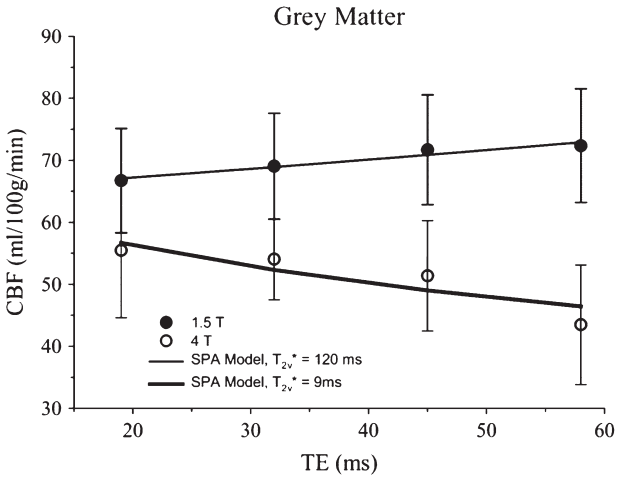

FIGURE 6. Cerebral blood flow data collected at 1.5 and 4 T plotted as a function of TE in gray matter. The best fit of the SPA model and the corresponding estimate of *T2v** are displayed for both field strengths. Error bars represent SEM.

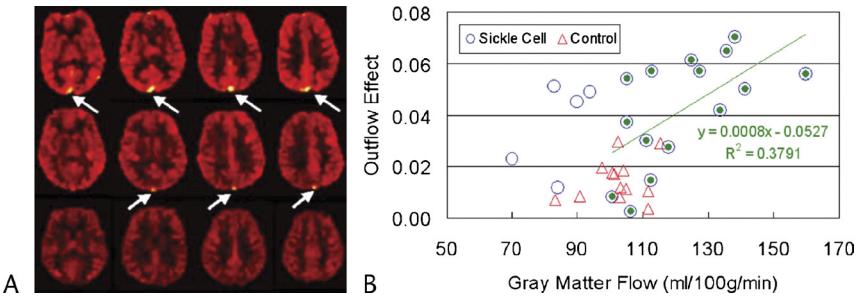

FIGURE 7. Cerebral blood flow images obtained from 3 representative subjects (A). Four slices are shown for each subject. From top to bottom: A child with a diagnosis of SCD, a healthy child, and a healthy adult. Arrows indicate hyperintensities in the sagittal sinus. Scatter plot of venous outflow effect versus gray matter blood flow (B); circled dots are data points with gray matter CBF >100 mL/100 g per minute that were used for regression analysis. Figure 7 can be viewed online in color at www.topicsinmri.com.

Thus, caution needs to be exercised when applying ASL to cases with high flow rate (eg, children, tumors, and hypercapnia) and/or prolonged blood T1 (eg, high magnetic field and children), although outflow effects may not be observable in healthy adults at 3.0 T. An interesting clinical application that uses the venous outflow effect is a recent ASL study on arteriovenous malformation.[58] Because of the direct shunt between arteries and veins, the labeled blood directly flows into veins causing intravenous hyperintensities similar to arterial transit artifacts. These intravenous hyperintensities in ASL images can be used to delineate and quantify the shunted flow through an arteriovenous malformation.

Other Factors Affecting Perfusion Quantification

The magnetization of blood in Equation [1], M_{0b}, is generally estimated from the measured signal of white matter by using the proton density ratio as well as T2 differences between blood and white matter.[53] To correct for coil inhomogeneity effects, a minimum contrast image (between gray matter, white matter, and cerebrospinal fluid) can be acquired by optimizing imaging parameters such as TR and TE.[59] An alternative approach to calculate M_{0b} is through scaling raw image intensity with the blood/tissue water partition coefficient (λ), although potential spatial variations of λ are a concern for accurate perfusion quantification in different tissue types (eg, gray and white matter).

Because of the lengthy acquisitions to achieve adequate SNR, ASL scans are susceptible to motion artifacts, especially in clinical settings such as stroke imaging. Nevertheless, recent technical advances offer several solutions to circumvent such limitation. The temporal fluctuations of ASL image series can be greatly reduced by placing inversion pulses to suppress the raw image intensity to as low as 1% of its original level—a technique termed background suppression.[60–62] More recently, "snapshot" ASL imaging capability (acquisition time <1 minute) has been demonstrated by combing background suppression, 3D acquisition, and pCASL.[63] This technique is expected to improve the robustness of ASL for clinical scans. With increasing use of ASL for body perfusion MRI, background suppression, synchronized breathing, and prospective gating techniques will find wider use in various applications.[64,65]

SUMMARY

Based on the above analyses, we recommend the following ASL imaging protocol for clinical perfusion MRI, with a total scan time of less than 10 minutes:

ASL Perfusion MRI Scanning Protocol	
pCASL scan	3–4 min
M0 and minimum contrast images	30 s
Blood T1	1 min
PC MRI at labeling plane	1 min
FEAST or multi-TI transit mapping	2–3 min
Total	9–10 min

The priority of the proposed sequences generally decreases from top to bottom. The PC MRI and transit time mapping sequences may be skipped as limited by time. Nevertheless, it will always pay off to run pilot scans in a representative patient population to estimate the arterial transit time and labeling efficiency for accurate perfusion quantification in formal studies. Although some of the listed sequences may be specific for our studies, pCASL and variant versions of transit time and T1 measurement sequences are available on MR systems of the 3 major vendors. It is to be hoped that this review will raise the awareness of potential issues in perfusion quantification using ASL especially in clinical populations and stimulate novel approaches for in vivo calibration of these factors.

REFERENCES

1. Wolf RL, Detre JA. Clinical neuroimaging using arterial spin-labeled perfusion magnetic resonance imaging. *Neurotherapeutics*. 2007;4:346–359.
2. Wang J, Rao H, Detre JA. Arterial spin labeling perfusion MRI in developmental neuroscience. In: *Neuroimaging in Developmental Clinical Neuroscience*. Rumsey JM, Ernst M, eds. Cambridge: Cambridge University Press; 2009:326–343.
3. Mai VM, Berr SS. MR perfusion imaging of pulmonary parenchyma using pulsed arterial spin labeling techniques: FAIRER and FAIR. *J Magn Reson Imaging*. 1999;9:483–487.
4. De Bazelaire C, Rofsky NM, Duhamel G, et al. Arterial spin labeling blood flow magnetic resonance imaging for the characterization of metastatic renal cell carcinoma. *Acad Radiol*. 2005;12:347–357.
5. Martirosian P, Klose U, Mader I, et al. FAIR true-FISP perfusion imaging of the kidneys. *Magn Reson Med*. 2004;51:353–361.
6. Zhang H, Shea SM, Park V, et al. Accurate myocardial T1 measurements: toward quantification of myocardial blood flow with arterial spin labeling. *Magn Reson Med*. 2005;53:1135–1142.

7. Detre JA. Clinical applicability of functional MRI. *J Magn Reson Imaging*. 2006;23:808–815.
8. Petersen ET, Mouridsen K, Golay X. The QUASAR reproducibility study. Part II: results from a multi center arterial spin labeling test-retest study. *Neuroimage*. 2010;49:104–113.
9. Friedman L, Stern H, Brown GG, et al. Test-retest and between-site reliability in a multicenter fMRI study. *Hum Brain Mapp*. 2008;29:958–972.
10. Friedman L, Glover GH. Reducing interscanner variability of activation in a multicenter fMRI study: controlling for signal-to-fluctuation-noise-ratio (SFNR) differences. *Neuroimage*. 2006;33:471–481.
11. Wong EC, Buxton RB, Frank LR. Implementation of quantitative perfusion imaging techniques for functional brain mapping using pulsed arterial spin labeling. *NMR Biomed*. 1997;10:237–249.
12. Alsop DC, Detre JA. Multisection cerebral blood flow MR imaging with continuous arterial spin labeling. *Radiology*. 1998;208:410–416.
13. Garcia DM, de Bazelaire C, Alsop D. Pseudo-continuous flow driven adiabatic inversion for arterial spin labeling. *Proc Int Soc Magn Reson Med*. 2005;13:37.
14. Wu WC, Fernandez-Seara M, Detre JA, et al. A theoretical and experimental investigation of the tagging efficiency of pseudocontinuous arterial spin labeling. *Magn Reson Med*. 2007;58:1020–1027.
15. Dai W, Garcia D, de Bazelaire C, et al. Continuous flow-driven inversion for arterial spin labeling using pulsed radio frequency and gradient fields. *Magn Reson Med*. 2008;60:1488–1497.
16. Wong EC, Cronin M, Wu WC, et al. Velocity-selective arterial spin labeling. *Magn Reson Med*. 2006;55:1334–1341.
17. Wu WC, Edlow BL, Elliot MA, et al. Physiological modulations in arterial spin labeling perfusion magnetic resonance imaging. *IEEE Trans Med Imaging*. 2009;28:703–709.
18. Wong EC, Buxton RB, Frank LR. A theoretical and experimental comparison of continuous and pulsed arterial spin labeling techniques for quantitative perfusion imaging. *Magn Reson Med*. 1998;40:348–355.
19. Buxton RB. Quantifying CBF with arterial spin labeling. *J Magn Reson Imaging*. 2005;22:723–726.
20. Chalela JA, Alsop DC, Gonzalez-Atavalez JB, et al. Magnetic resonance perfusion imaging in acute ischemic stroke using continuous arterial spin labeling. *Stroke*. 2000;31:680–687.
21. Alsop DC, Detre JA. Reduced transit-time sensitivity in noninvasive magnetic resonance imaging of human cerebral blood flow. *J Cereb Blood Flow Metab*. 1996;16:1236–1249.
22. Wang J, Alsop DC, Li L, et al. Comparison of quantitative perfusion imaging using arterial spin labeling at 1.5 and 4.0 tesla. *Magn Reson Med*. 2002;48:242–254.
23. Buxton RB, Frank LR, Wong EC, et al. A general kinetic model for quantitative perfusion imaging with arterial spin labeling. *Magn Reson Med*. 1998;40:383–396.
24. Parkes LM, Tofts PS. Improved accuracy of human cerebral blood perfusion measurements using arterial spin labeling: accounting for capillary water permeability. *Magn Reson Med*. 2002;48:27–41.
25. Zhou J, Wilson DA, Ulatowski JA, et al. Two-compartment exchange model for perfusion quantification using arterial spin tagging. *J Cereb Blood Flow Metab*. 2001;21:440–455.
26. St Lawrence KS, Frank JA, McLaughlin AC. Effect of restricted water exchange on cerebral blood flow values calculated with arterial spin tagging: a theoretical investigation. *Magn Reson Med*. 2000;44:440–449.
27. Li KL, Zhu X, Hylton N, et al. Four-phase single-capillary stepwise model for kinetics in arterial spin labeling MRI. *Magn Reson Med*. 2005;53:511–518.
28. Ye FQ, Berman KF, Ellmore T, et al. H(2)(15)O PET validation of steady-state arterial spin tagging cerebral blood flow measurements in humans. *Magn Reson Med*. 2000;44:450–456.
29. Feng CM, Narayana S, Lancaster JL, et al. CBF changes during brain activation: fMRI vs. PET. *Neuroimage*. 2004;22:443–446.
30. Siewert B, Schlaug G, Edelman RR, et al. Comparison of EPISTAR and T2*-weighted gadolinium-enhanced perfusion imaging in patients with acute cerebral ischemia. *Neurology*. 1997;48:673–679.
31. Weber MA, Gunther M, Lichy MP, et al. Comparison of arterial spin-labeling techniques and dynamic susceptibility-weighted contrast-enhanced MRI in perfusion imaging of normal brain tissue. *Invest Radiol*. 2003;38:712–718.
32. Wolf RL, Alsop DC, McGarvey ML, et al. Susceptibility contrast and arterial spin labeled perfusion MRI in cerebrovascular disease. *J Neuroimaging*. 2003;13:17–27.
33. Wang J, Aguirre GK, Kimberg DY, et al. Arterial spin labeling perfusion fMRI with very low task frequency. *Magn Reson Med*. 2003;49:796–802.
34. Floyd TF, Ratcliffe SJ, Wang J, et al. Precision of the CASL-perfusion MRI technique: global and regional cerebral blood flow within vascular territories at one hour and one week. *J Magn Reson Imaging*. 2003;18:649–655.
35. Yen YF, Field AS, Martin EM, et al. Test-retest reproducibility of quantitative CBF measurements using FAIR perfusion MRI and acetazolamide challenge. *Magn Reson Med*. 2002;47:921–928.
36. Parkes LM, Rashid W, Chard DT, et al. Normal cerebral perfusion measurements using arterial spin labeling: reproducibility, stability, and age and gender effects. *Magn Reson Med*. 2004;51:736–743.
37. Wang J, Licht DJ, Silverstre DW, et al. Why perfusion in neonates with congenital heart defects is negative?—Technical issues related to pulsed arterial spin labeling. *Magn Reson Imaging*. 2006;24:249–254.
38. Wong EC, Buxton RB, Frank LR. Quantitative imaging of perfusion using a single subtraction (QUIPSS and QUIPSS II). *Magn Reson Med*. 1998;39:702–708.
39. Wang J, Zhang Y, Wolf RL, et al. Amplitude modulated continuous arterial spin labeling perfusion MR with single coil at 3T-feasibility study. *Radiology*. 2005;235:218–228.
40. Aslan S, Xu F, Wang PL, et al. Estimation of labeling efficiency in pseudocontinuous arterial spin labeling. *Magn Reson Med*. 2010;63:765–771.
41. Jain V, Giannetta M, Langham M, et al. Precision and accuracy of arterial spin labeling perfusion MRI in the pediatric population. *Proc Int Soc Magn Reson Med*. 2010;18:2040.
42. Petersen ET, Lim T, Golay X. Model-free arterial spin labeling quantification approach for perfusion MRI. *Magn Reson Med*. 2006;55:219–232.
43. Yang Y, Engelien W, Xu S, et al. Transit time, trailing time, and cerebral blood flow during brain activation: measurement using multislice, pulsed spin-labeling perfusion imaging. *Magn Reson Med*. 2000;44:680–685.
44. Wu WC, Wang J, Detre JA, et al. Transit delay and flow quantification in muscle with continuous arterial spin labeling perfusion-MRI. *J Magn Reson Imaging*. 2008;28:445–452.
45. Chen J, Licht DJ, Smith S, et al. Arterial spin-labeling perfusion MRI in pediatric arterial ischemic stroke—initial experiences. *J Magn Reson Imaging*. 2009;29:282–290.
46. Wang J, Alsop DC, Song HK, et al. Arterial transit time imaging with flow encoding arterial spin tagging (FEAST). *Magn Reson Med*. 2003;50:599–607.
47. Gunther M, Bock M, Schad LR. Arterial spin labeling in combination with a Look-Locker sampling strategy: inflow turbo-sampling EPI-FAIR (ITS-FAIR). *Magn Reson Med*. 2001;46:974–984.

48. Hendrikse J, van Osch MJ, Rutgers DR, et al. Internal carotid artery occlusion assessed at pulsed arterial spin-labeling perfusion MR imaging at multiple delay times. *Radiology*. 2004;233:899–904.
49. Dai W, Robson PM, Shankaranarayanan A, et al. ASL perfusion measurement using a rapid, low resolution arterial transit time prescan. *Proc Int Soc Magn Reson Med*. 2009;17:625.
50. Wu WC, Jain V, Li C, et al. In vivo venous blood T(1) measurement using inversion recovery true-FISP in children and adults. *Magn Reson Med*. 2010;64:1140–1147.
51. St Lawrence KS, Wang J. Effects of the apparent transverse relaxation time on cerebral blood flow measurements obtained by arterial spin labeling. *Magn Reson Med*. 2005;53:425–433.
52. Wolf RL, Wang J, Wang S, et al. Grading of CNS neoplasms using continuous arterial spin labeled perfusion MR. *J Magn Reson Imaging*. 2005;22:475–482.
53. Warmuth C, Gunther M, Zimmer C. Quantification of blood flow in brain tumors: comparison of arterial spin labeling and dynamic susceptibility-weighted contrast-enhanced MR imaging. *Radiology*. 2003;524:523–532.
54. Wang J, Fernandez-Seara MA, Wang S, et al. When perfusion meets diffusion: in vivo measurement of water permeability in human brain. *J Cereb Blood Flow Metab*. 2007;27:839–849.
55. Wu WC, Rao H, Pawlak MA, et al. Venous outflow of label in ASL perfusion MRI of healthy children and children with sickle cell disease. *Proc Int Soc Magn Reson Med*. 2008;16:2054.
56. Wang J, Licht DJ. Pediatric perfusion MRI with arterial spin labeling. *Neuroimaging Clin N Am*. 2006;16:149–167.
57. Oguz KK, Golay X, Pizzini FB, et al. Sickle cell disease: continuous arterial spin-labeling perfusion MR imaging in children. *Radiology*. 2003;227:567–574.
58. Wolf RL, Wang J, Detre JA, et al. Arteriovenous shunt visualization in arteriovenous malformations with arterial spin-labeling MR imaging. *AJNR Am J Neuroradiol*. 2008;29:681–687.
59. Wang J, Qiu M, Constable RT. In vivo method for correcting transmit/receive nonuniformities with phased array coils. *Magn Reson Med*. 2005;53:666–674.
60. Garcia DM, Duhamel G, Alsop DC. Efficiency of inversion pulses for background suppressed arterial spin labeling. *Magn Reson Med*. 2005;54:366–372.
61. Ye FQ, Frank JA, Weinberger DR, et al. Noise reduction in 3D perfusion imaging by attenuating the static signal in arterial spin tagging (ASSIST). *Magn Reson Med*. 2000;44:92–100.
62. St Lawrence KS, Frank JA, Bandettini PA, et al. Noise reduction in multi-slice arterial spin tagging imaging. *Magn Reson Med*. 2005;53:735–738.
63. Fernandez-Seara MA, Edlow BL, Hoang A, et al. Minimizing acquisition time of arterial spin labeling at 3T. *Magn Reson Med*. 2009;59:1467–1471.
64. Robson PM, Madhuranthakam AJ, Dai W, et al. Strategies for reducing respiratory motion artifacts in renal perfusion imaging with arterial spin labeling. *Magn Reson Med*. 2009;61:1374–1387.
65. Wang DJ, Bi X, Avants BB, et al. Estimation of perfusion and arterial transit time in myocardium using free-breathing myocardial arterial spin labeling with navigator-echo. *Magn Reson Med*. 2010;64:1289–1295.